Materials Research Proceedings 57 (2025) 199-207 https://doi.org/10.21741/9781644903735-23

Impact of cell dimensions and beam radius on the bending characteristics of BCC sandwich panels produced via L-PBF of Ti6Al4V

Dina PALMERI[1,a *], Gaetano POLLARA[1,b], Gianluca BUFFA[1,c] and Livan FRATINI[1,d]

[1]Università Degli studi di Palermo, Dipartimento di Ingegneria, Viale delle Scienze, 90128 Palermo, Italia

[a]dina.palmeri@unipa.it, [b]gaetano.pollara@unipa.it, [c]gianluca.buffa@unipa.it, [d]livan.fratini@unipa.it

Keywords: Laser Powder Bed Fusion, Ti6Al4V, BCC Sandwich Panels, Three-Point Bending Tests

Abstract. Ti-6Al-4V lattice structures created through Laser Powder Bed Fusion L-PBF find extensive use in sandwich panels for applications that demand both high strength and lightweight characteristics, particularly in aerospace and biomedical fields. L-PBF technology provides significant design flexibility, enabling the fabrication of complex geometry and modification of lattice mechanical properties to meet specific requirements. Understanding the correlation among unit cell type, relative density, unit cell arrangement, and mechanical properties is essential for the design of effective lattice structures. The aim of the study was to examine how the panel's behaviour varied with changes in the two body centered cubic (BCC) cell parameters cell size and beam radius. The samples produced were evaluated mechanically through the carrying out of three-point bending tests. Simulations of the additive process were conducted to emphasize the existence of residual stresses, connecting with the findings from previous tests.

Introduction

Additive manufacturing (AM) has grown in popularity in recent years because to its ability to produce highly customizable parts, lightweight structures, and multifunctional components [1, 2]. This is especially true in the aerospace sector, where lightweight constructions result in reduced buy-to-fly ratios and cost savings during the product's useful life [3]. In this case, a metal lattice structure can be beneficial in reducing the weight of the component while retaining high strength [4]. Lattice structures are formed by the repeating of a basic cell, which can be strut-based or mathematically structured to achieve zero-mean curvature at all points on the surface (triply periodic minimum surface, or TPMS) [5]. In the first scenario, the unit cell is basically defined by two geometrical properties: cell size and beam radius, which determine the mechanical response of the lattice [6, 7]. Recently, BCC lattice structures have been investigated for metal lattice sandwich panels (MLSPs) with anti-icing or energy absorption applications [8, 9]. Ti-6Al-4V can be used to print MLSPs, especially in aerospace applications where good mechanical properties and corrosion resistance are requested. Since a high resolution is needed to print small features, such as the struts within the unit cell, laser powder bed fusion (LPBF) is the most suitable among AM technologies for metals [10].

Few studies can be found in the literature on MLSPs made of a lattice core and a solid skin. Acanfora et al. [9] analyzed the influences of different BCC cell configurations on the shock-absorbing capacity of hybrid sandwich panels made of an additive-manufactured metal lattice core and composite skins. The impact response of these panels has been investigated through FEM analysis and validated with some literature studies. The results confirm the reduction of the mass

Content from this work may be used under the terms of the Creative Commons Attribution 3.0 license. Any further distribution of this work must maintain attribution to the author(s) and the title of the work, journal citation and DOI. Published under license by Materials Research Forum LLC.

and the increase in the shock-absorbing capacity by using a lattice core with respect to the reference literature test case. FEM analysis was carried out also by Wey et al. [11] to assess the blast response of Ti-6Al-4V Auxetic honeycomb sandwich panels manufactured with LPBF. They demonstrate that AM sandwich panels can be used for modern protective structures for enhanced blast resistance. Li et al. [12] investigated multi-layer lattice panels' compressive modulus and crushing strength with body-centered cubic with vertical strut (BCCZ) cells. AlSi10Mg panels fabricated via LPBF were subjected to compressive tests. FEM analysis was used to predict the compressive response of multi-layer lattice panels. The results show that the lattice panels' layer and cell number strongly affect the entire structure's mechanical response. Kang et al. [13] proposed a multi-lattice design for stainless steel 630 panels using both BCC and octet-truss lattice structures. The topology optimization was performed to obtain the minimum relative density. Three-point bending tests were used to validate the proposed method and to compare the new design with the traditional uniform lattice structures. The new design leads to an increase in the panel's stiffness and a different deformation mode. The compression failure of AlSi10Mg trabecular structures has been analyzed by Ferro et al. [14]. Two different structures, BCC and BCCZ, were printed by LPBF and tested. The effect of cell shape, strut, and cell dimension was studied to establish the best design for the final application. From this study, the most influential factors are the cell shape and cell dimension.

The literature review shows a lack of studies on the mechanical behavior of Ti-6Al-4V lattice sandwich panels, especially on their flexural strength, by changing the geometrical cell characteristics. This paper analyzes the effect of unit cell size and beam radius on the flexural response of Ti-6Al-4V MLSPs through three-point bending tests.

Materials and Methods

The objective of the study was to analyze the behavior of the MLSPs, built with L-PBF technology, by modifying two cell parameters: cell size and beam radius. Specifically, two distinct values were selected for the two parameters, while maintaining the sample dimensions (see Fig. 1a). After establishing the dimensions of the samples, the subsequent values for cell size and beam radius were selected:

Cell size: 2 mm - 3 mm;

Beam Radius: 0.25 mm - 0.35 mm.

Based on the aforementioned geometric characteristics, the characterized samples have been designated as C2 - R0.25, C2 - R0.35, C3 - R0.25, and C3 - R0.35. Depending on the selected geometric parameters, each panel was also characterized by the V_f (Volume fraction) parameter, which indicates the ratio between the volume of the panel and the volume of the sample considered as full. This metric indicates the extent of weight reduction provided by the examined lattice configuration. The samples were fabricated by means of L-PBF technique with Ti-6Al-4V grade 23 alloy, which has minimal interstitial components including oxygen and iron, resulting in favorable ductility and strength characteristics. The longitudinal orientation of the samples was selected to align with the z-building direction to reduce panel distortions. A gas-atomized spherical powder was utilized for the studies. The particle size exhibits a Gaussian distribution, with d10 and d90 values of 20µm and 63µm, respectively. The employed process parameters are those recommended by SLM Solutions for Ti-6Al-4V powder. Laser power is set at P=350 W, scanning speed at v=1400 mm/s, layer thickness at t=30 µm, and hatch distance at h=120 µm. The diameter of the laser beam focus was established at 100 µm. The employed scan strategy combines hatching and contour, with the scanning direction rotated by 15° on the plane for each layer. The Build Plate temperature is maintained at 200 °C to reduce thermal gradients.

The mechanical behavior of MLSP was evaluated using three-point bending tests. Samples were manufactured in accordance with the ASTM E290 standard, with dimensions of 80 mm in length (L), 13 mm in height (H), and 12 mm in width (W), with the lattice core region (refer to

Materials Research Proceedings 57 (2025) 199-207 https://doi.org/10.21741/9781644903735-23

Fig. 1) possessing a cross-sectional area of 12 mm x 12 mm. Three-point bending tests were conducted using a Galdabini Quasar 600 universal testing machine at a constant velocity of 0.5 mm/min.

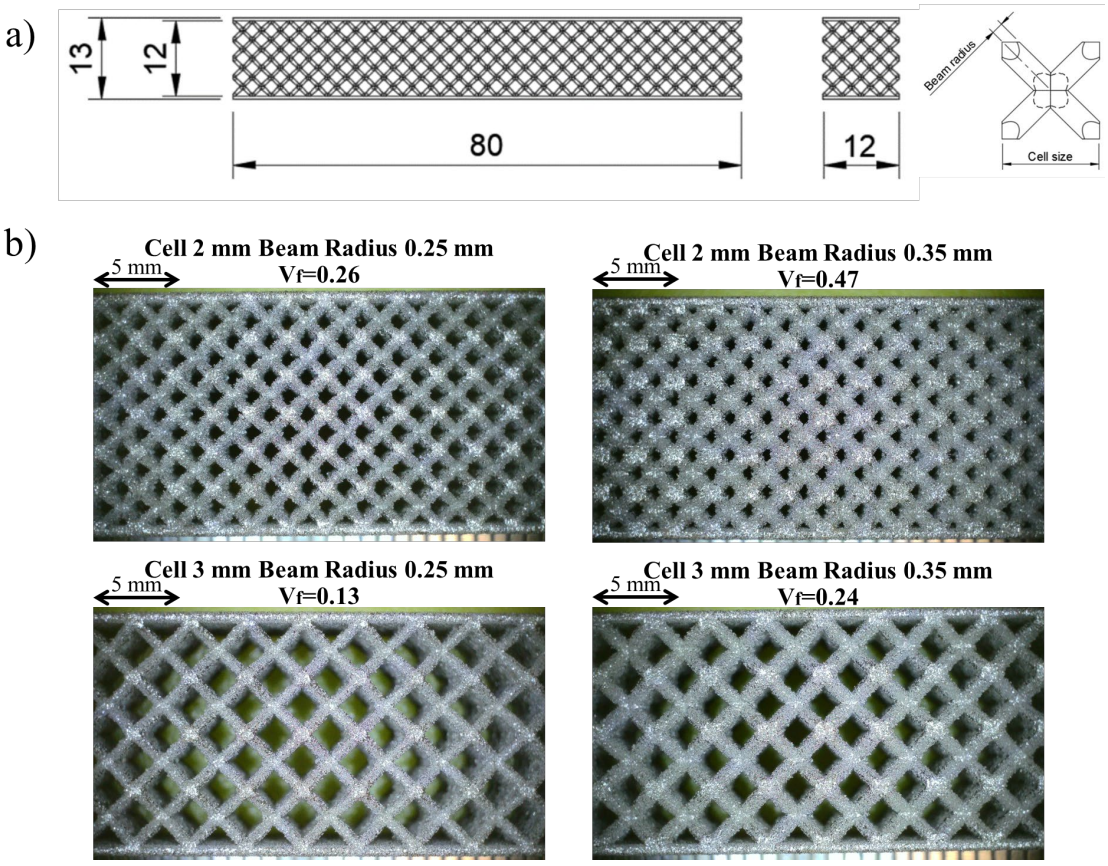


Figure 1. a) Samples dimensions for three-point bending test in accordance with the ASTM E290 standard, length L=80 mm, height H=13 mm, and width W=12 mm, b) Printed lattice samples with varying geometric characteristics.

In addition to the mechanical assessments of the samples through the use of three-point bending tests, the additive process was simulated in order to discover any significant dimensional mismatches that existed between the geometry that was planned and the geometry that was ultimately obtained. Through the use of simulations, it was possible to determine the distribution of residual stresses that were generated throughout the additive process. These findings were then correlated with the strength that was found in the individual samples. Numerical simulations were conducted with Netfabb Simulation (Autodesk) to study distortions and residual stress distributions along the building direction (z) during the L-PBF process of Ti-6Al-4V on the MLSPs. Correlation analyses were performed between the results of additive simulations and the outcomes of experimental tests, specifically focusing on the lattice region of the sandwich panels.

To carry out the numerical simulation, it is essential to create a parameter file (PRM) containing the mesoscale information required for the part-scale simulation. The PRM file must specify what is being used 3D printing machine, material characteristics, and scanning procedure. Consequently, a calibration step for the model is unneeded [15].

Results and Discussions

The results of the three-point bending tests allowed the characterization of the strength of the MLSPs. The acquired data concerned the load and stroke of the punch, from which all the useful

Materials Research Proceedings 57 (2025) 199-207 https://doi.org/10.21741/9781644903735-23

data and graphs for comparing the panels characterized by different geometric parameters were then obtained. Furthermore, the test was enhanced with the acquisition of images to analyze the deformation of the sample and, where possible, the progression of the crack (phenomena that vary significantly among the different types of samples).

In the following Fig.2, the results of the mechanical characterization tests of the sandwich panels with BCC lattice core structure are reported. As can be observed from Fig. 2 and the photo acquisitions shown in Fig. 3 for the C2 specimens, both in the case of R0.25 and in the case of R0.35, after a slight deflection, there is a brittle fracture with an unstable crack propagation, which opens in mode I, that is, by tension. For the C3 specimens, a completely different behavior is observed. The panel initially behaves as if it were subjected to compression, as the load is transferred to the core with a punch penetration; thereafter, it also breaks with a mode I crack. This behavior occurs for a beam radius of 0.25, while for R0.35, a behavior similar to that previously described for the C2 panels is restored.

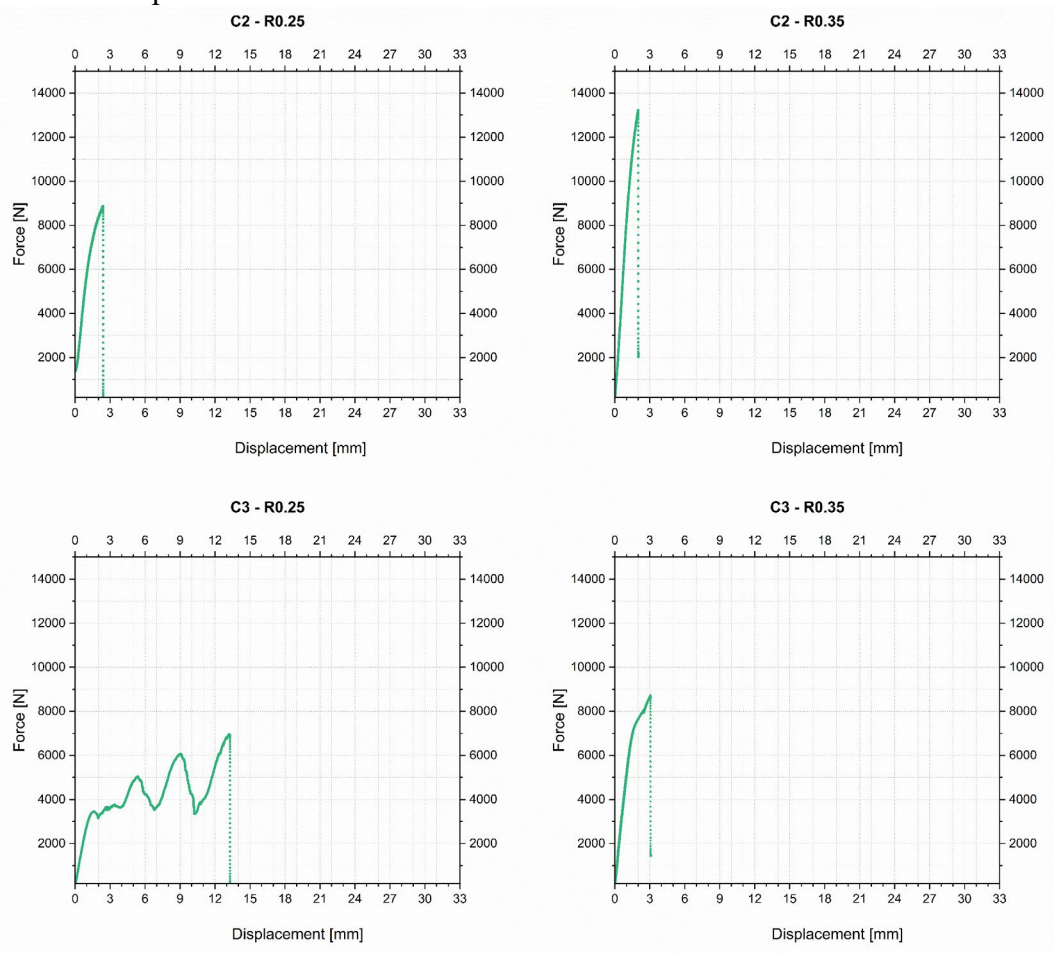


Figure 2. Three point bending test results: maximum load to failure [N] and punch displacement [mm].

Materials Research Proceedings 57 (2025) 199-207 https://doi.org/10.21741/9781644903735-23

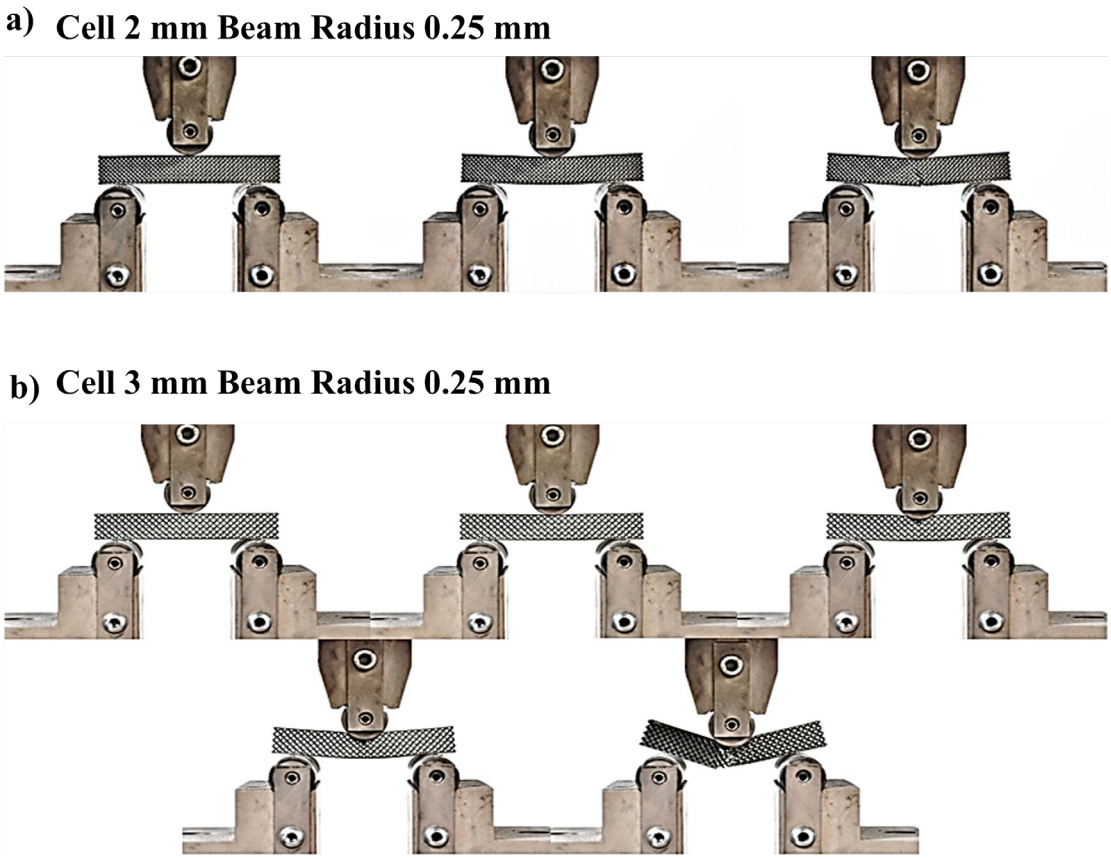


Figure 3. Photographic acquisitions during the three-point bending test. a) panels with cell size equal to 2 mm and beam radius 0.25 mm b) panel with cell size 3 mm and beam radius 0.25 mm.

The results indicated that as cell size increases and V_f decreases, it is feasible, in certain instances, to preserve the strength of a panel with a smaller cell size, thereby enhancing ductility and achieving a lightweight effect on the sandwich panel. This condition was observed for moderate reductions in V_f. For V_f values significantly lower than those held by the C2-R0.25 and C2-R0.35 panels, the MLSPs experience a considerable reduction in resistance.

The numerical simulations of additive manufacturing, the results of which are presented in Fig. 4 and Fig. 5 as the size of the unit cell changes, have emphasized that the additive process does not cause major variations between the design geometry and the geometry actually produced.

A higher variation is found in the panels characterized by the 2 mm cell, notably in the first printed layers. Such deviation affects a slightly larger area of the sample in the case where the beam radius is greater while keeping the cell size constant. The residual stresses linked to the additive process in the z-direction indicate that an increase in beam radius for a cell size of 2 mm results in a substantial rise in compressive forces in the longitudinal mid-section of the samples. This stress distribution enhances the strength as indicated in Fig. 2. For an elementary cell with a higher dimension (C3 mm), an increase in beam radius consistently results in increased residual compressive stresses within the longitudinal section of the panel along the z-axis. This impact is, however, less strong than in the previous scenario.

Materials Research Proceedings 57 (2025) 199-207 https://doi.org/10.21741/9781644903735-23

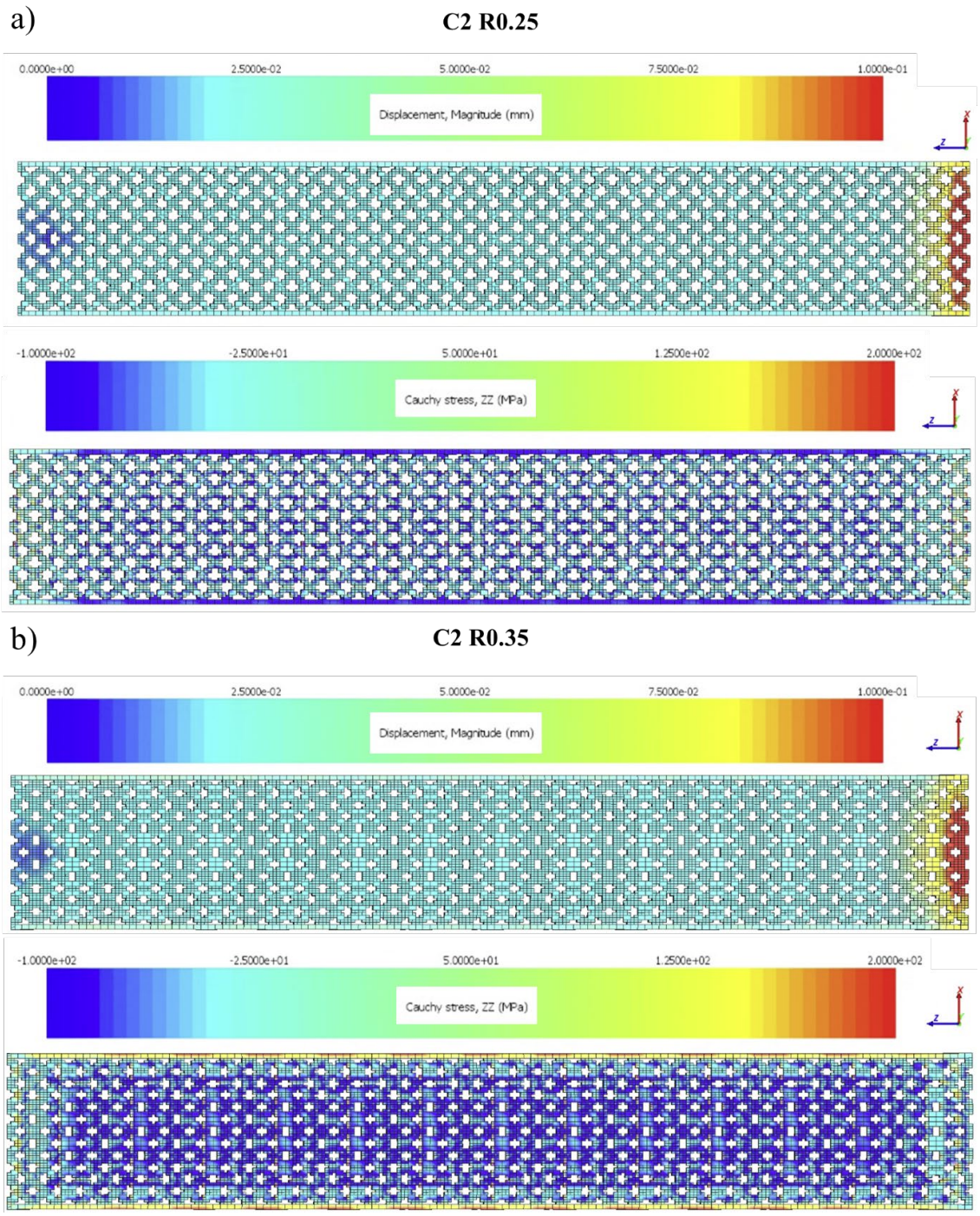


Figure 4. Numerical simulation of L-PBF process results. a) displacement and residual stress along the z direction for the panel C2 – R0.25, b) displacement and residual stress along the z direction for the panel C2 – R0.35.

Materials Research Proceedings 57 (2025) 199-207 https://doi.org/10.21741/9781644903735-23

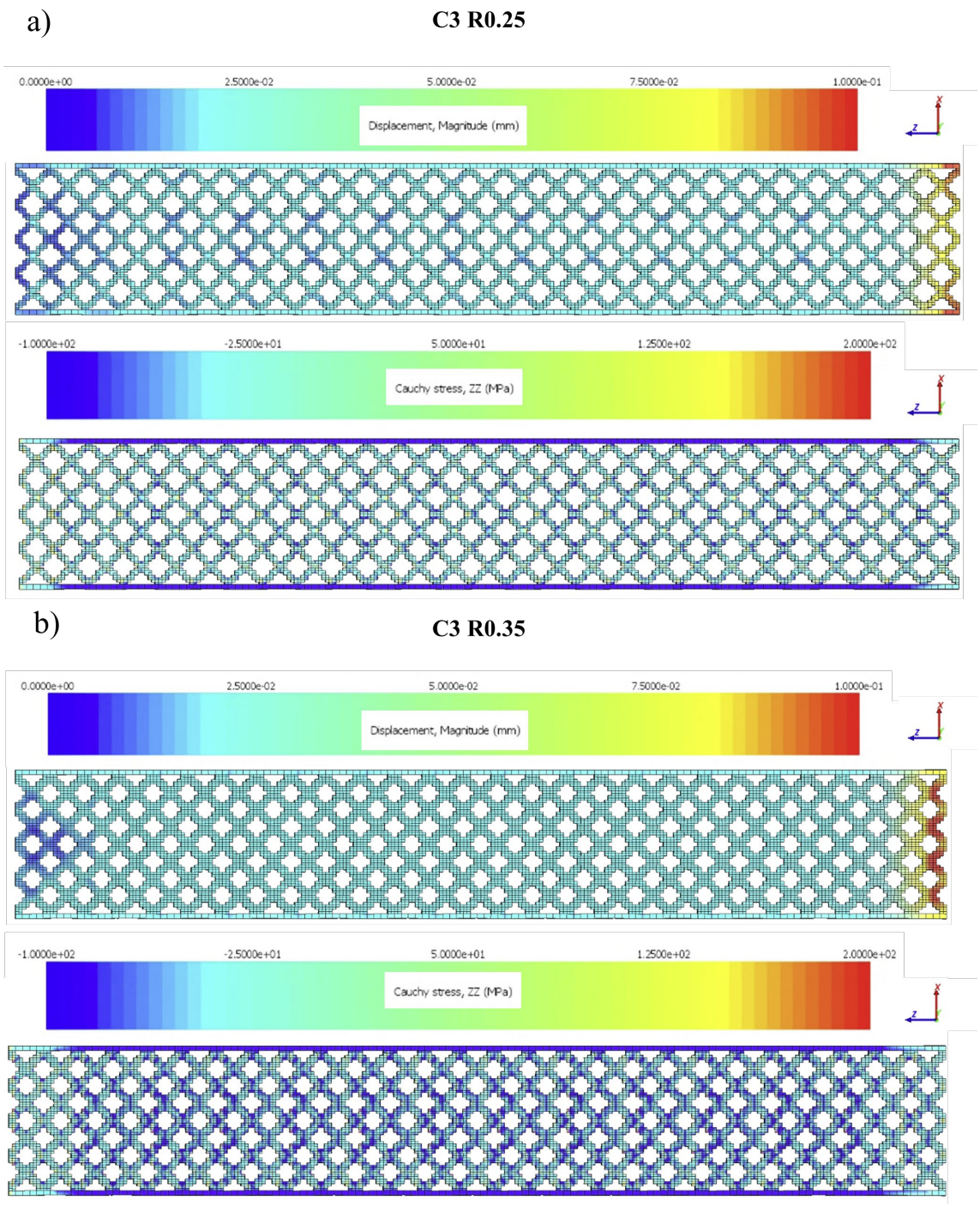


Figure 5. Numerical simulation of L-PBF process results. a) displacement and residual stress along the z direction for the panel C3 – R0.25, b) displacement and residual stress along the z direction for the panel C3 – R0.35.

The growth of beam radius in the 3 mm cell results in a longitudinal distribution of residual stresses similar to the C2 – R0.25 scenario. This situation results in a bending resistance for the C3 – R0.35 sample comparable to that of the C2 – R0.25 example, but with an enhancement in ductility due to the decrease in the V_f parameter.

Conclusions

In this paper, the mechanical properties of BCC MLSPs produced by L-PBF technology at the varying of two body centered cubic cell parameters as the cell size and the beam radius are investigated. Three-point bending tests and a numerical model of the process allowed the prediction of the residual stresses and distortions in the BCC MLSPs and the mechanical characterization of the panels as the geometry of the lattice core varies.

Based on the main findings, it can be concluded that:

- For the C2 specimens, after a small deflection, there is a brittle fracture with an unstable crack propagation, which opens in mode I, that is, by tension. This occurs in both the case of R0.25 and the case of R0.35, respectively. The behavior of the C3 specimens is shown to be entirely different from what was seen. As the load is carried to the core by a punch penetration, the panel first exhibits the behavior of a panel that has been exposed to compression. Subsequently, the panel likewise fractures with a mode I crack. The behavior described here takes place when the beam radius is 0.25, however when the radius is 0.35, a behavior that is comparable to the one that was described before for the C2 panels is restored.
- As the cell size grows and the value of V_f decreases, the findings suggested that it is possible, in some circumstances, to maintain the strength of a panel with a smaller cell size. This would result in an increase in ductility and the achievement of a lightweight effect on the sandwich panel.
- The numerical simulations of additive manufacturing show that the design geometry and the geometry produced are not significantly different.
- Continuously increasing beam radius increases residual compressive stresses in the longitudinal panel section along the z-axis. This effect decreases with cell size increasing.

References

[1] Guo N, Leu MC (2013) Additive manufacturing: Technology, applications and research needs. Frontiers of Mechanical Engineering 8:215–243. https://doi.org/10.1007/s11465-013-0248-8

[2] Herzog D, Seyda V, Wycisk E, Emmelmann C (2016) Additive manufacturing of metals. Acta Mater 117:371–392. https://doi.org/10.1016/j.actamat.2016.07.019

[3] Blakey-Milner B, Gradl P, Snedden G, et al (2021) Metal additive manufacturing in aerospace: A review. Mater Des 209:. https://doi.org/10.1016/j.matdes.2021.110008

[4] Soro N, Saintier N, Merzeau J, et al (2021) Quasi-static and fatigue properties of graded Ti–6Al–4V lattices produced by Laser Powder Bed Fusion (LPBF). Addit Manuf 37:101653. https://doi.org/10.1016/j.addma.2020.101653

[5] AlMahri S, Santiago R, Lee D-W, et al (2021) Evaluation of the dynamic response of triply periodic minimal surfaces subjected to high strain-rate compression. Addit Manuf 46:102220. https://doi.org/10.1016/j.addma.2021.102220

[6] Riva L, Ginestra PS, Ceretti E (2021) Mechanical characterization and properties of laser-based powder bed–fused lattice structures: a review. The International Journal of Advanced Manufacturing Technology 113:649–671

[7] Chen L-Y, Liang S-X, Liu Y, Zhang L-C (2021) Additive manufacturing of metallic lattice structures: Unconstrained design, accurate fabrication, fascinated performances, and challenges. Materials Science and Engineering: R: Reports 146:100648. https://doi.org/10.1016/j.mser.2021.100648

[8] Bici M, Brischetto S, Campana F, et al (2018) Development of a multifunctional panel for aerospace use through SLM additive manufacturing. Procedia CIRP 67:215–220. https://doi.org/10.1016/j.procir.2017.12.202

[9] Acanfora V, Saputo S, Russo A, Riccio A (2021) A feasibility study on additive manufactured hybrid metal/composite shock absorbers. Compos Struct 268:113958. https://doi.org/10.1016/j.compstruct.2021.113958

[10] Liu S, Shin YC (2019) Additive manufacturing of Ti6Al4V alloy: A review. Mater Des 164:. https://doi.org/10.1016/j.matdes.2018.107552

[11] Wei Y, Zhang C, Yuan Y, et al (2023) Blast response of additive manufactured Ti–6Al–4V sandwich panels. Int J Impact Eng 176:104553. https://doi.org/10.1016/j.ijimpeng.2023.104553

[12] Li C, Lei H, Liu Y, et al (2018) Crushing behavior of multi-layer metal lattice panel fabricated by selective laser melting. Int J Mech Sci 145:389–399. https://doi.org/10.1016/j.ijmecsci.2018.07.029

[13] Kang D, Park S, Son Y, et al (2019) Multi-lattice inner structures for high-strength and light-weight in metal selective laser melting process. Mater Des 175:107786. https://doi.org/10.1016/j.matdes.2019.107786

[14] Ferro CG, Varetti S, Maggiore P, et al (2020) Design and characterization of trabecular structures for an anti-icing sandwich panel produced by additive manufacturing. Journal of Sandwich Structures & Materials 22:1111–1131. https://doi.org/10.1177/1099636218780513

[15] Peter N, Pitts Z, Thompson S, Saharan A. Benchmarking build simulation software for laser powder bed fusion of metals. Addit Manuf 2020;36:101531. https://doi.org/10.1016/j.addma.2020.101531